Loss rate of ultracold neutrons due to the absorption by trap walls

Pavel D. Grigoriev & Vladislav D. Kochev

[1]L. D. Landau Institute for Theoretical Physics, Chernogolovka, Russia
[2]National University of Science and Technology "MISiS", Moscow, Russia

Plan of the talk:

1. **Introduction and motivation. Experiments with ultracold neutrons (UCN).**
2. **Our calculations of the UCN loss rate**
3. **Difference between the vertical and horizontal UCN motion and its influence on energy and geometry extrapolation procedures.**
4. **Dependence of the geometry extrapolation on the UCN trap shape.**
5. **Conclusions.**

ISINN-30

Neutron Decay

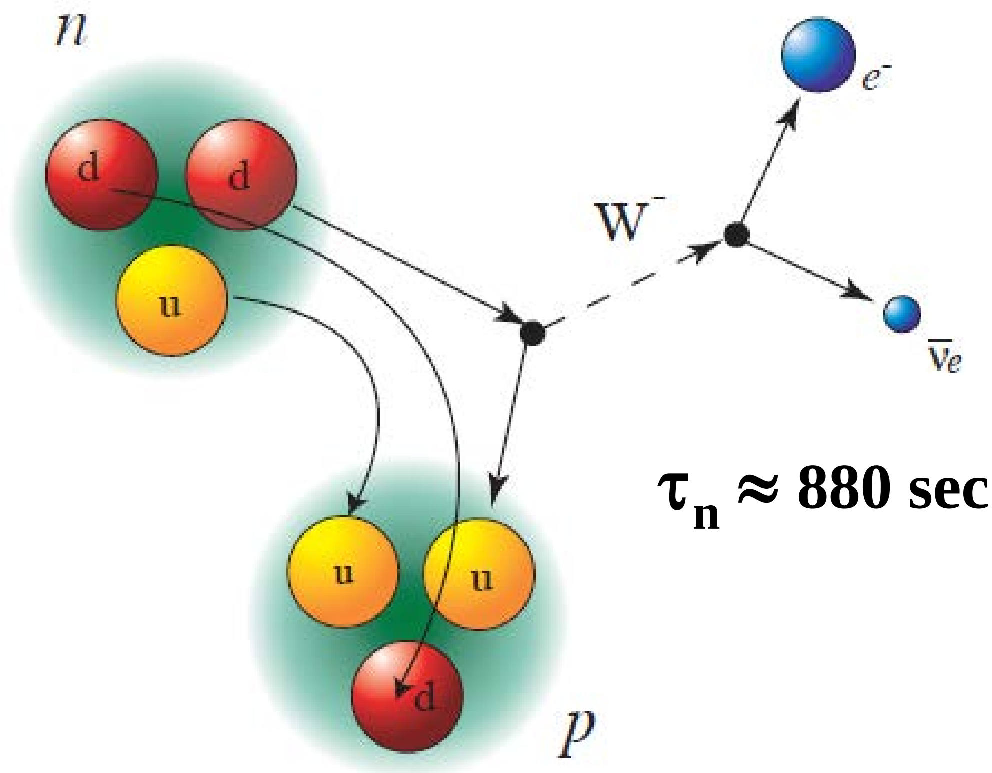

$\tau_n \approx$ **880 sec ≈ 15 minutes**

$$n \rightarrow p^+ + e^- + \bar{\nu}_e + 782\ \mathrm{keV}$$

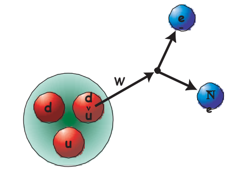

Importance of Neutron Decay Parameters

- τ_n: Big Bang Nucleosynthesis - determines primordial helium abundance
- g_V: determines V_{ud}, test of CKM unitarity
- g_A: axial vector coupling in weak decays
- D: search for new CP violation

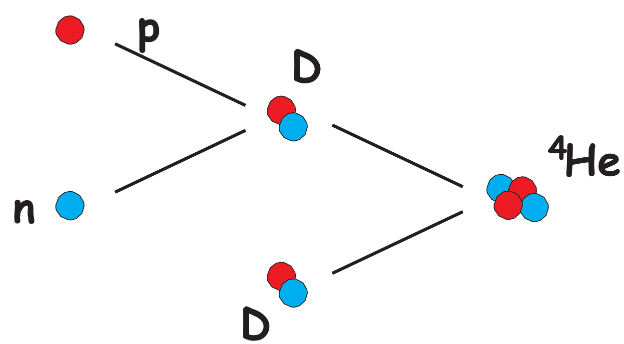

- a, A, B: precise comparison is sensitive to non-SM physics:
  - right handed currents
  - scalar and tensor forces
  - CVC violation
  - second class currents

Cabibbo–Kobayashi–Maskawa matrix

$$\begin{pmatrix} d' \\ s' \\ b' \end{pmatrix} = \begin{pmatrix} V_{ud} & V_{us} & V_{ub} \\ V_{cd} & V_{cs} & V_{cb} \\ V_{td} & V_{ts} & V_{tb} \end{pmatrix} \begin{pmatrix} d \\ s \\ b \end{pmatrix}$$

Big Bang Nucleosynthesis

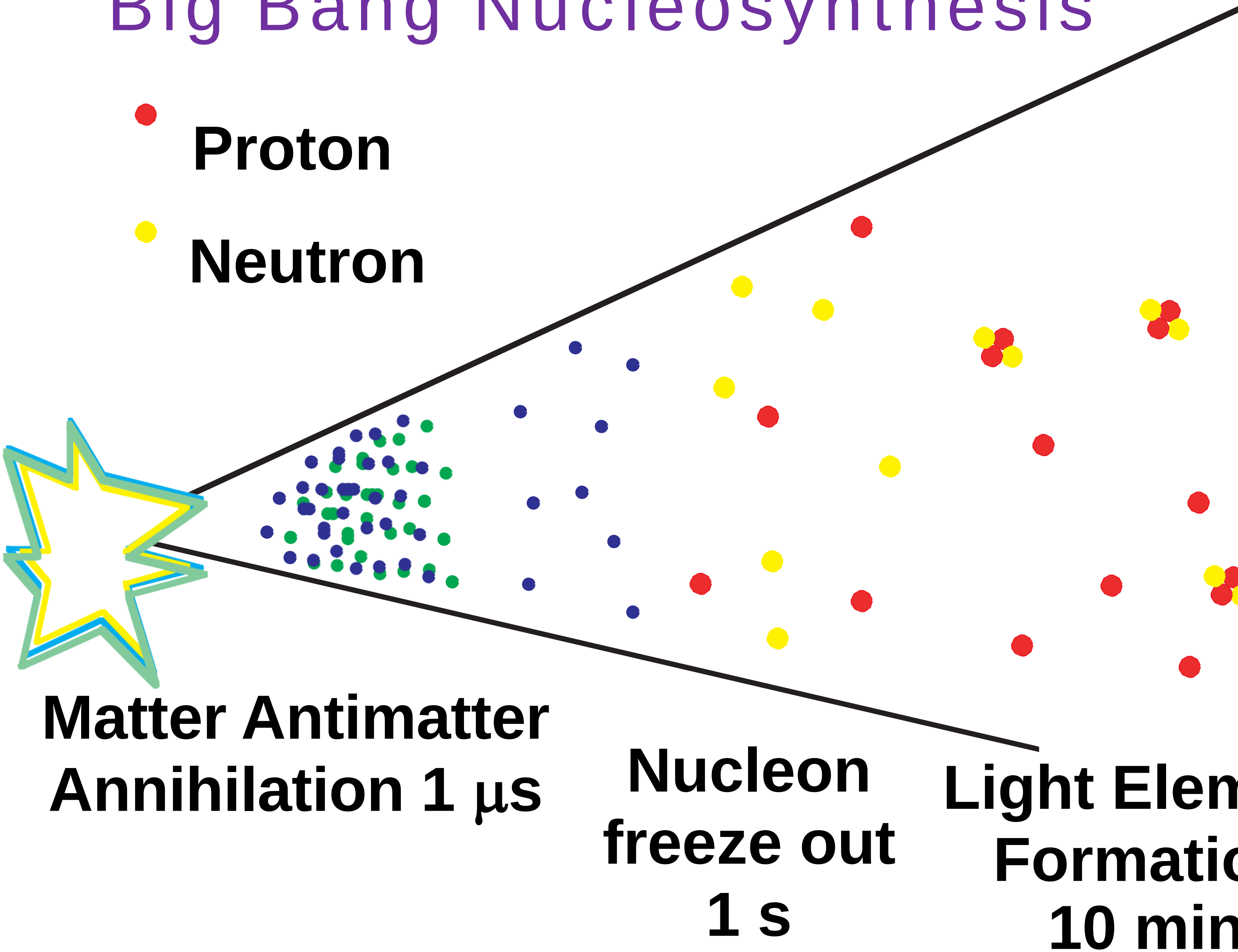

CKM unitarity (Cabibbo–Kobayashi–Maskawa matrix)

- $|V_{us}|$ and $|V_{ub}|$ obtained from high-energy experiments

- $|V_{ud}|$ obtained from:
  1. $0^+ \rightarrow 0^+$ nuclear beta decay
  2. neutron beta decay
  3. pion beta decay

As of 2020, the magnitudes of the CKM matrix elements are

Zyla et al. (Particle Data Group) (2020). "Review of Particle Physics: CKM quark-mixing matrix" *Progress of Theoretical and Experimental Physics*. 2020 (8): 083C01.

$$\begin{bmatrix} |V_{ud}| & |V_{us}| & |V_{ub}| \\ |V_{cd}| & |V_{cs}| & |V_{cb}| \\ |V_{td}| & |V_{ts}| & |V_{tb}| \end{bmatrix} = \begin{bmatrix} 0.97370 \pm 0.00014 & 0.2245 \pm 0.0008 & 0.00382 \pm 0.00024 \\ 0.221 \pm 0.004 & 0.987 \pm 0.011 & 0.0410 \pm 0.0014 \\ 0.0080 \pm 0.0003 & 0.0388 \pm 0.0011 & 1.013 \pm 0.030 \end{bmatrix}$$

$$|V_{\mathrm{ud}}|^2 + |V_{\mathrm{us}}|^2 + |V_{\mathrm{ub}}|^2 = 0.9985 \pm 0.0005$$

g_A and g_V (definition)

At the quark level the hadronic current is written as a mixture of vector and axial-vector parts: $J_H^\mu = \bar{u}(x)\gamma^\mu(1-\gamma_5)d(x)$

Renormalization effects of strong interactions give the hadronic current between nucleons (neutron n and proton p) rather complex form

$$J_H^\mu = \bar{p}(x)[V^\mu - A^\mu]n(x),$$

where the vector-current part $V^\mu = g_V(q^2)\gamma^\mu + \mathrm{i}g_M(q^2)\frac{\sigma^{\mu\nu}}{2m_N}q_\nu$

and the axial-vector-current part $A^\mu = g_A(q^2)\gamma^\mu\gamma_5 + g_P(q^2)q^\mu\gamma_5.$

Here $g_V(q^2) = \frac{g_V}{(1+q^2/M_V^2)^2}; g_A(q^2) = \frac{g_A}{(1+q^2/M_A^2)^2},$

$g_M(q^2) = (\mu_p - \mu_n)g_V(q^2)$ **and** $g_P(q^2) = 2m_N g_A(q^2)/(q^2+m_\pi^2),$

where M_V = 84 MeV and $M_A \sim$ 1GeV, m_π is the pion mass

$\mu_p - \mu_n = 3.70$ **is the anomalous magnetic moment of the nucleon.**

g_A and g_V

$$|V_{ud}| \propto g_v$$

$$\tau_n \propto \frac{1}{(g_v^2 + 3g_a^2)}$$

$$A = -2\frac{\lambda^2 + \lambda}{1 + 3\lambda^2}$$

$$\lambda = \frac{g_a}{g_v}$$

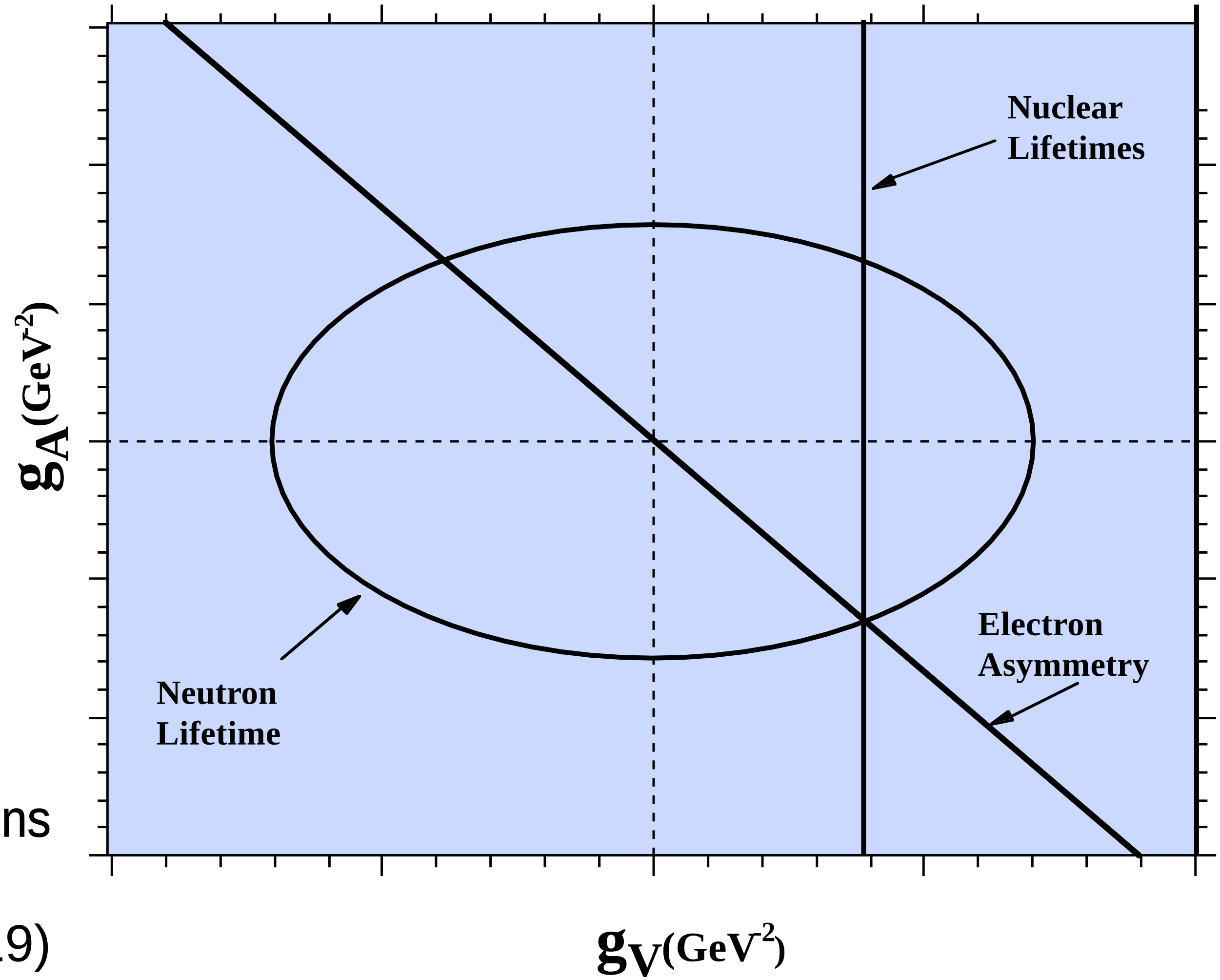

decay of polarized neutrons
B. Märkisch et al.,
PRL122, 242501 (2019)

$$\lambda = g_A/g_V = -1.27641(45)_{\text{stat}}(33)_{\text{sys}}$$

$$A_0 = -0.11985(17)_{\text{stat}}(12)_{\text{sys}}$$

g_A and g_V (various studies)

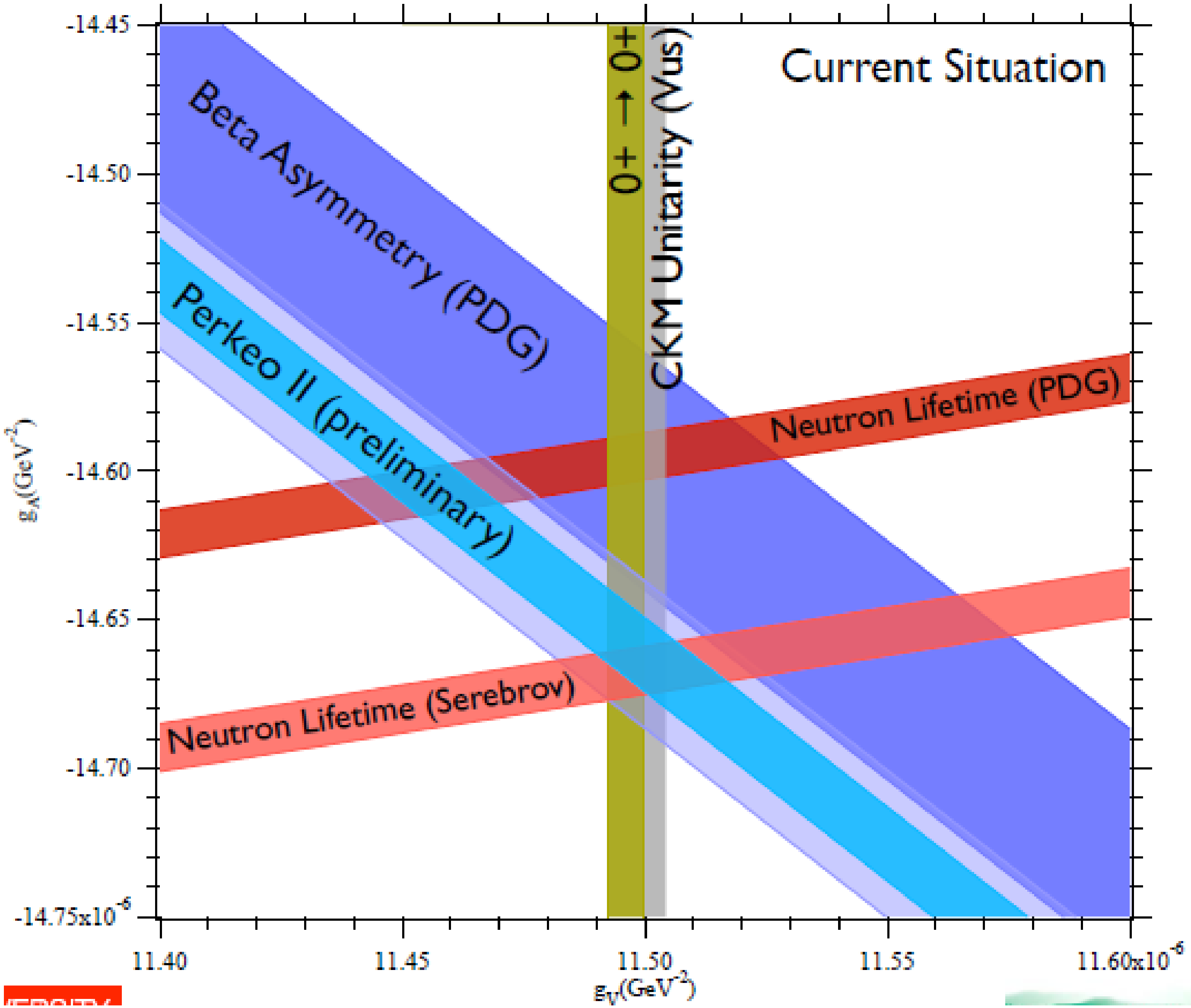

Electric dipole moment of elementary particles

Particle	Experimental limit (90% C.L.) (e cm)	Method employed in latest experiment
e	$<1.6 \times 10^{-27}$	Thallium beam [67]
μ	$<2.3 \times 10^{-19}$	Tilt of precession plane in anomalous magnetic moment experiment [68]
τ	$(-1.6 < d_\tau < 3.9) \times 10^{-17}$	Electric form factor in $e^+e^- \rightarrow \tau\tau$ events [69]
n	$<3.0 \times 10^{-26}$	Ultracold neutrons [70]
p	$(-3.7 \pm 6.3) \times 10^{-23}$	120 kHz thallium spin resonance [71]
Λ^0	$(-3.0 \pm 7.4) \times 10^{-17}$	Spin precession in motional electric field [72]
$\nu_{e,\mu}$	$<2 \times 10^{-21}$	Inferred from magnetic moment limits [73]
ν_τ	$<5.2 \times 10^{-17}$	Z decay width [74]
^{199}Hg	$<2.1 \times 10^{-28}$	Mercury atom spin precession [75]

1.1×10^{-29} *e*·cm (2018)

Taken from H.Abele, Progress in Particle and Nuclear Physics 60,1-81 (2008)

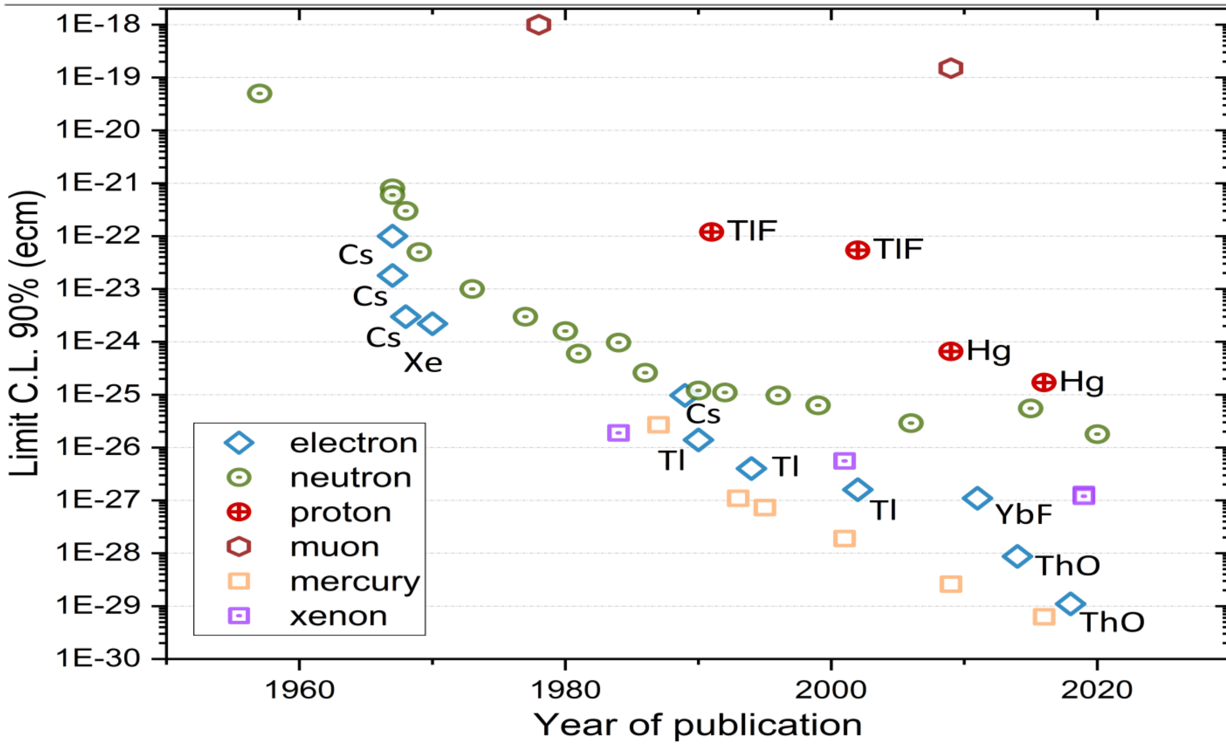

The neutron spin polarization precession frequency

$$h\nu = |2\mu_n B \pm 2d_n E|$$

Storage time of UCN may be important for EDM measurements via corrections to systematic errors, e.g. geometric phase

Energy Scales/Nomenclature

	Energy	Wavelength	Temperature	Velocity
Fast	> 500 keV			> 1 x 10^7 m/s
Epihermal	500 keV - 25 meV			1 x 10^7 m/s- 2200 m/s
Thermal	25 meV	0.18 nm	300 K	2200 m/s
Cold	25 meV - 0.05 meV	0.18 nm - 4 nm	300 K - 0.6 K	2200 m/s - 100 m/s
Very Cold	50 μeV - 0.2 μeV	4 nm - 64 nm	0.6 K - 0.002 K	100 m/s - 6 m/s
Ultracold	< 0.2 μeV	> 64 nm	< 2 mK	< 6 m/s

Types of neutron lifetime measurements

Technique		Challenges
❶ **Neutron Beam** Detect decay products from a beam with a well defined neutron fluence rate	$-dN/dt = N\lambda$	Absolute neutron flux (10^{-3})
❷ **Material Bottle** Measure change in number of confined neutrons as a function of time	The gravitational potential of 100 neV/m	Understanding neutron energy spectrum Loss mechanisms (walls)
❸ **Magnetic Bottle** Measure change in number of confined neutrons as a function of time	$N_1/N_2 = e^{-\lambda(t_1 - t_2)}$ neutron magnetic moment creates a potential 60 neV/T	Complicated Orbits Spin Flips
❹ **Magnetic Trap** Count decay products of magnetically trapped neutrons as a function of time and measure the slope.	$ln(N/N_0) = -\lambda t$	Complicated Orbits To date: poor signal to noise Nonuniform magnetic field => spin flip

Measurement Summary (last 35 years)

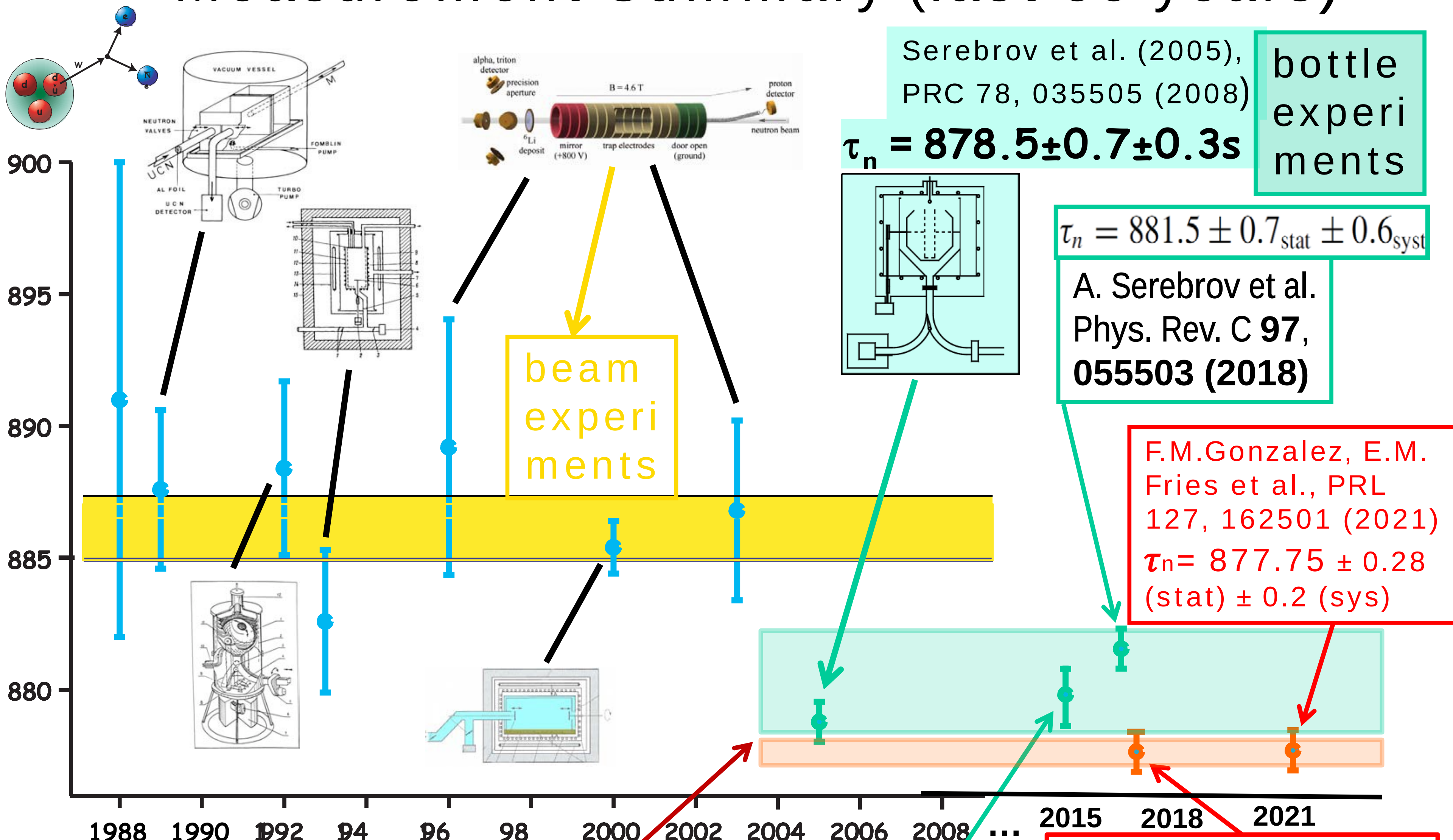

The discrepancy between τ_n measured using different techniques (neutron lifetime puzzle) is also between magnetic and material traps

Arzumanov et al. (2015)

Magnetic trap

τ_n = **877.7** ± 0.7 (stat) +0.4/–0.2(sys)

Pattie et al., Science 360, 627 (2018)

Neutron lifetime measurements using superfluid helium 4 covering trap walls – the only material which does not absorb neutrons at all

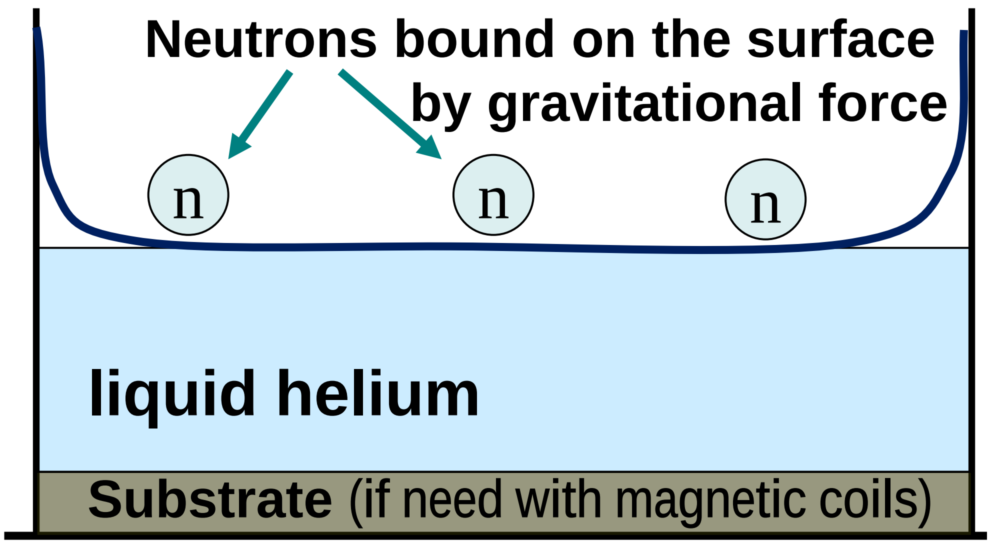

Unfortunately, the side trap walls are covered by only very thin **~10nm superfluid helium film on a height** $h > h_0 = \sqrt{2} a_{\mathrm{He}} \sqrt{1 - \sin\theta}$ **where the capillary length of** ^4He

$$a_{\mathrm{He}} = \sqrt{\sigma_{\mathrm{He}} / g \rho_{\mathrm{He}}} = 0.5 \quad \mathrm{mm}$$

The maximal height of UCN with $E < V_0 = 18.5$neV is $h_{max} = 18$cm.

Our proposal: to use surface roughness & electric field to increase the thickness of superfluid helium

Phys. Rev. C 104, 055501 (2021)
JETP Letters 114(8), 493 (2021)
Phys. Rev. C 108, 025501 (2023)

1D triangular

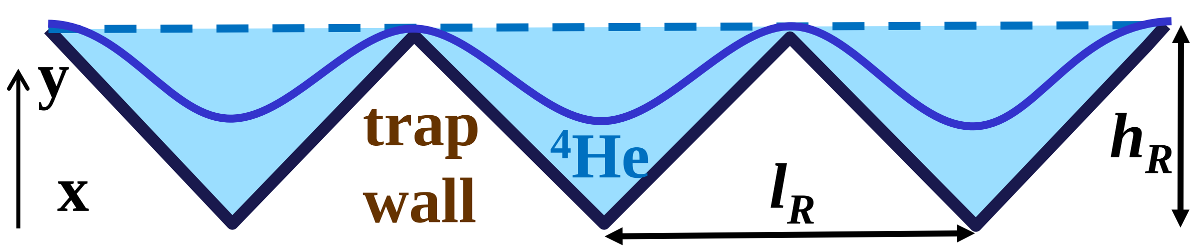

History of measurements for last 20 years

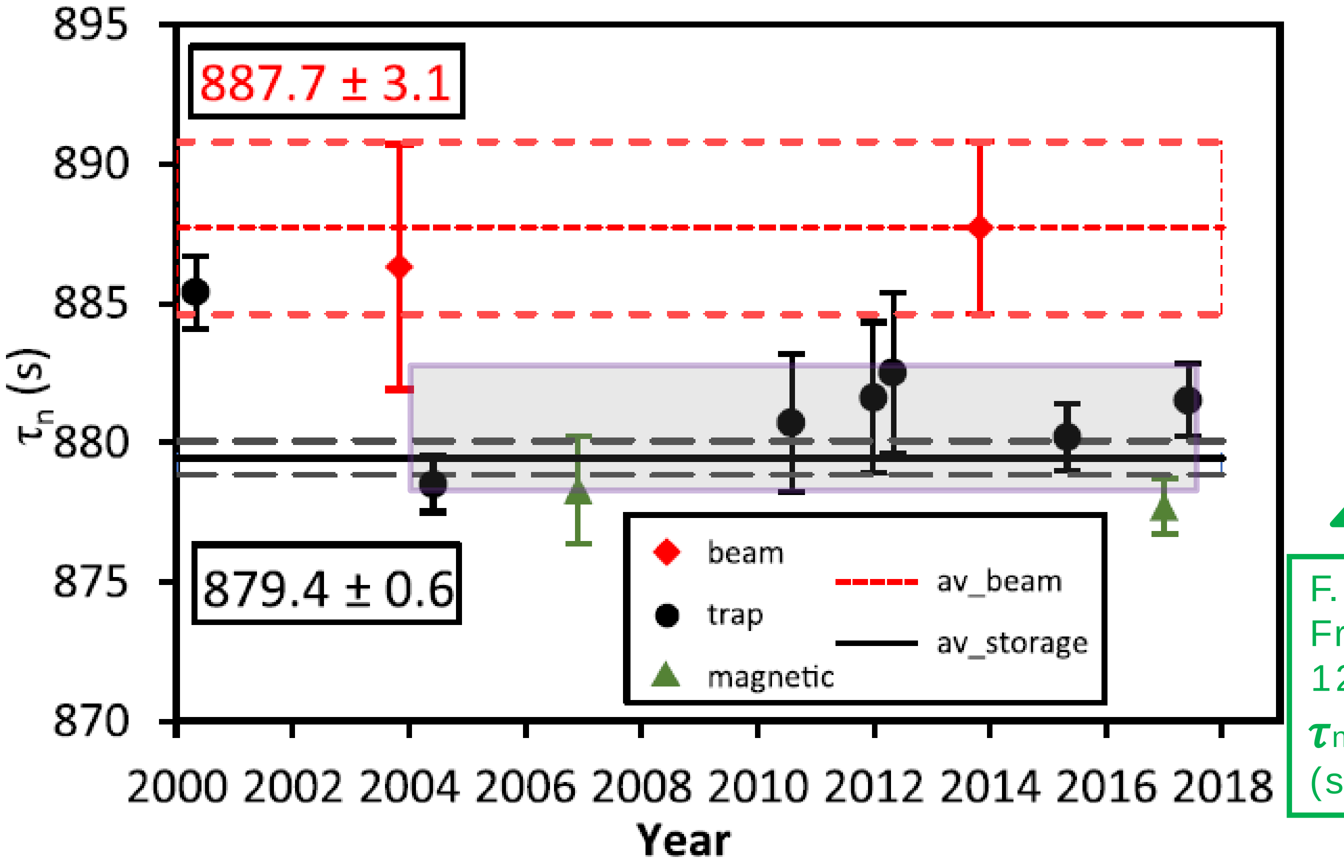

F.M.Gonzalez, E.M. Fries et al., PRL 127, 162501 (2021)
τ_n= 877.75 ± 0.28 (stat) ± 0.2 (sys)

The discrepancy between τ_n measured using different techniques (neutron lifetime puzzle) is also between magnetic and material traps

In A. P. Serebrov et al., Phys. Rev. D 103, 074010 (2021) a discussion of possible errors in beam experiments is given, but there is also a difference between bottle and magnetic-trap measurements, much beyond the claimed errors.

Neutron lifetime measurements with a large gravitational trap (Serebrov et al., 2018)

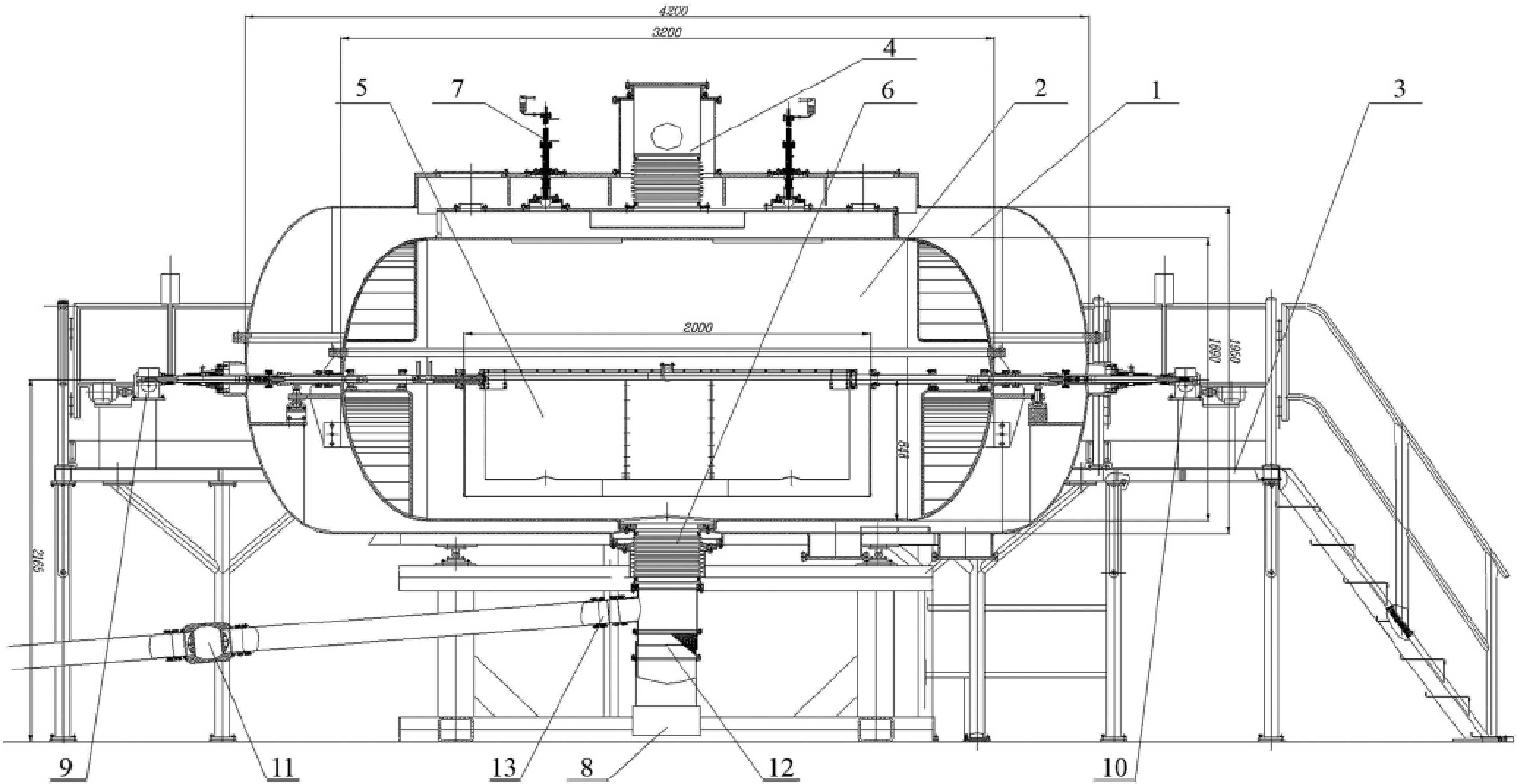

FIG. 2. 1 external vacuum vessel, 2–internal vacuum vessel, 3–platform for service, 4–gear for pumping out internal vessel, 5–trap with insert in low position, 6–neutron guide system, 7–system of coating of trap and insert, 8–detector, 9–mechanism for turning trap, 10–mechanism for turning insert, 11–turbine shutter, 12–detector shutter, 13–neutron guide shutter.

Extrapolation interval to get free neutron lifetime is still about 20 s (Serebrov et al., 2018)

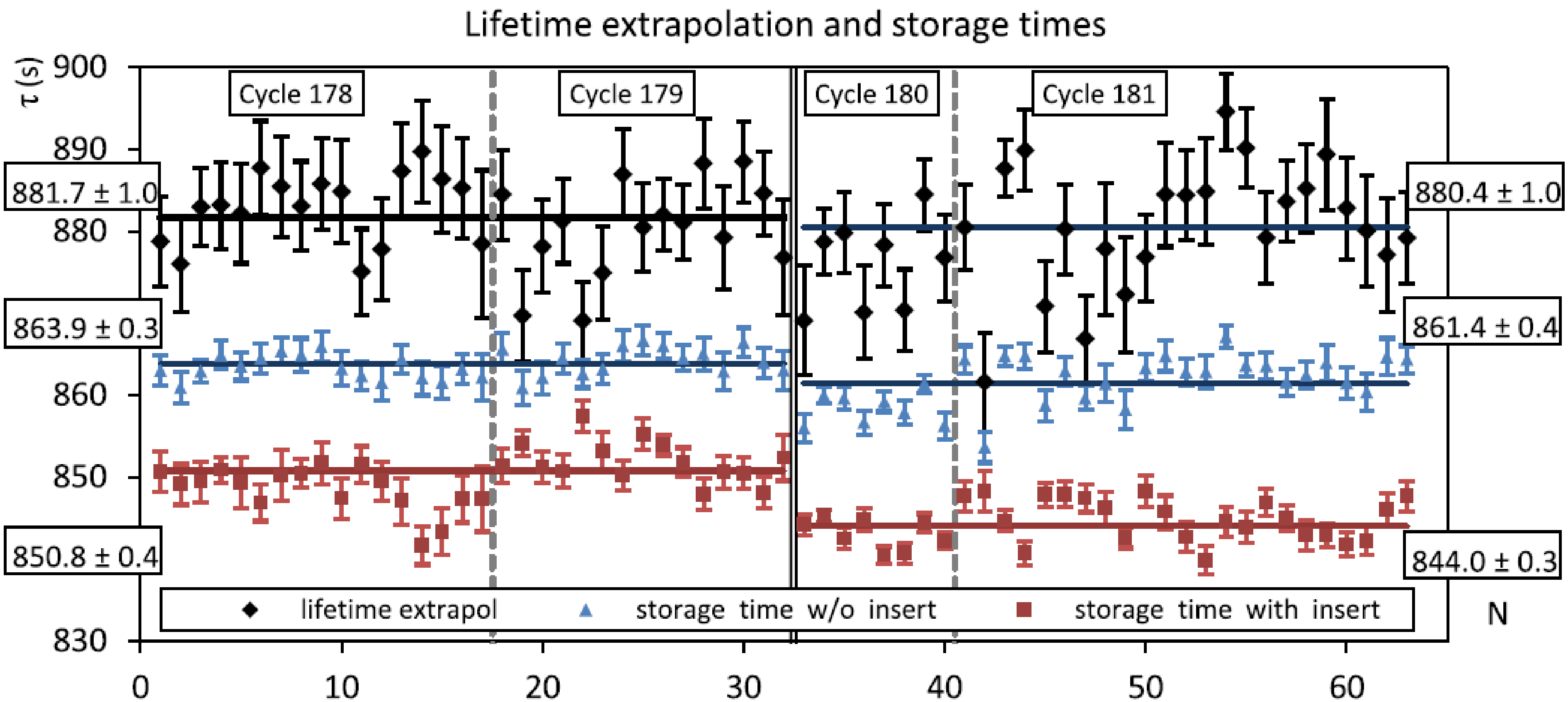

Time diagram showing successive measurements of the storage times and the corresponding extrapolated free neutron lifetime over the period of experiment. The vertical black solid line separates measurements with and without the titanium absorber, vertical dashed lines separate the reactor cycles.

UCN storage time extrapolations have uncertainty

Collision frequency ν(*E*) as a function of UCN energy *E*

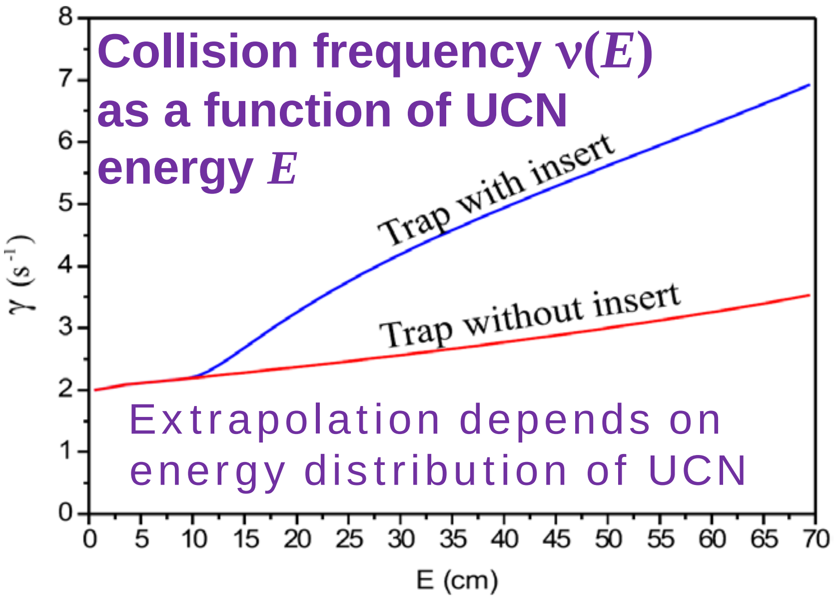

Extrapolation depends on energy distribution of UCN

$$\tau_{\text{loss}}^{-1} = \mu(T,E)\nu(E),$$ where $\boldsymbol{\mu(T,E)}$ is the probability that a UCN is lost at each collision, which depends on UCN energy and wall temperature

$$\mu(v_\perp) = \frac{2\eta x}{\sqrt{1-x^2}}, \quad \text{where } x = v_\perp / v_{lim}.$$

Usually one assumes isotropic distribution of UCN velocity and square wall barrier, giving

$$\mu(y) = \frac{2\eta}{y^2}\left(\arcsin y - y\sqrt{1-y^2}\right)$$ **where the UCN velocity** $y = \sqrt{E/U_0} = v/v_{lim}$

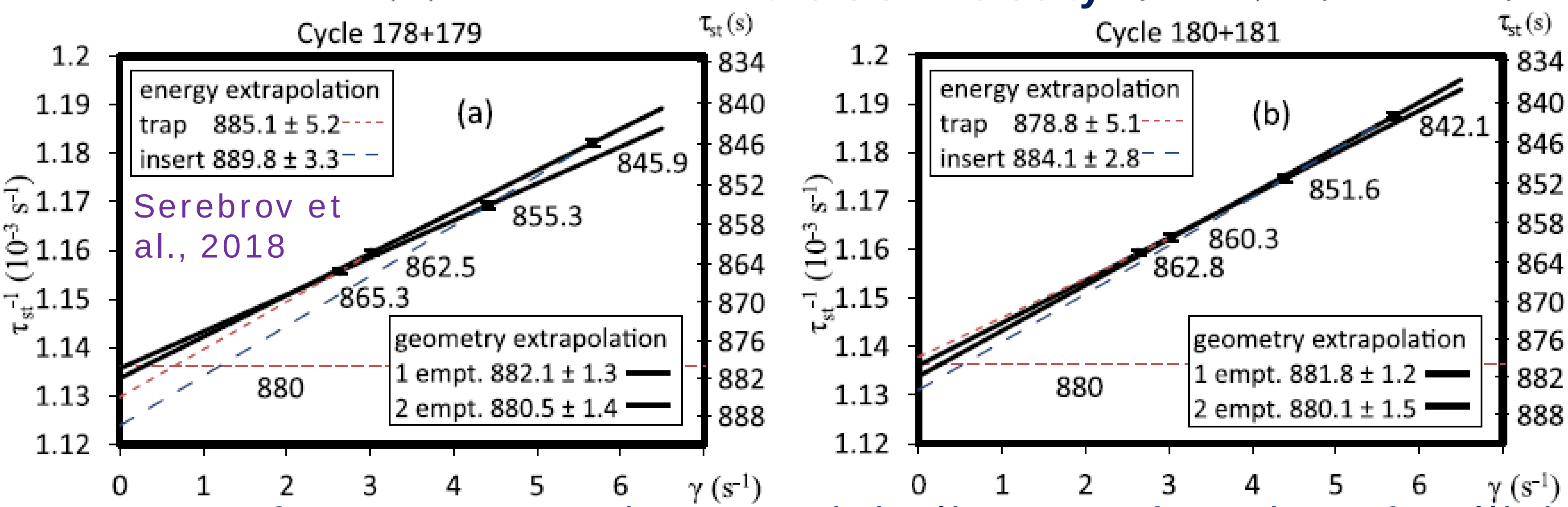

Serebrov et al., 2018

Loss rate of UCN may not be a straight line as a function of collision rate if the angular distribution of UCN velocity also changes.

! UCN storage time extrapolations have uncertainty

The UCN loss rate $\tau_{\text{loss}}^{-1} = \mu(T,E)\nu(E)$, where $\boldsymbol{\mu(T,E) \sim 10^{-5}}$ is the loss probability at each collision, which depends on UCN energy and wall temperature and $\boldsymbol{\nu(E) > 2s^{-1}}$ is the collision frequency.

For rectangular potential barrier $\mu(\upsilon_\perp) = \dfrac{2\eta x}{\sqrt{1-x^2}}$, where $x = \upsilon_\perp / \upsilon_{lim}$.

Usually, one assumes isotropic distribution of UCN velocity at any height:

$$\mu(y) = \frac{2\eta}{y^2}\left(\arcsin y - y\sqrt{1-y^2}\right)$$

where the total UCN velocity $y = \sqrt{E/U_0} = \upsilon/\upsilon_{lim}$

These assumptions disregard 1) the dependence of angular distribution of UCN velocity on height (which depends on trap and inset geometry); 2) the roughness of trap walls (which also changes the UCN angular distribution). 3) the energy distribution of UCN is not known. 4) the rate of UCN collisions with trap walls depends differently on horizontal and vertical components of UCN velocity. => the geometrical scaling fails.

While the real angular distribution of UCN velocity during collisions can be found using more difficult Monte-Carlo simulations, the uncertainty (systematic error) due to wall roughness is very difficult for modeling.

The gravity effect on the absorption rate

In the usual calculation of UCN losses the gravity only changes the UCN density & velocity absolute value (as a function of height) but not its angular distribution.

The UCN loss rate

$$\tau_{loss}^{-1}(E) = \frac{\int_0^{h_{\max}(E)} \bar{\mu}\left[E-h'\right] v\left(E-h'\right) \rho\left(E,h'\right)\, dS(h)}{4\int_0^{h_{\max}(E)} \rho\left(E,h'\right)\, dV(h)}$$

UCN absorption rate per bounce averaged over incidence angle

$$\bar{\mu}(E_k) = \frac{2\eta}{v_*^2}\left(\arcsin v_* - v_*\sqrt{1-v_*^2}\right) \approx \begin{cases} \pi\eta, & v_* \to 1, \\ 4\eta v_*/3, & v_* \ll 1, \end{cases}$$

UCN density and normalized velocity as a function of height

$$\rho(E,h) \propto \sqrt{\left(E-h'\right)/E} \qquad h' \equiv m_n g h$$

$$v_*(h) = \sqrt{\left(E-m_n g h\right)/V_0}$$

A. Serebrov et al. Phys. Rev. C **97**, **055503 (2018)**

It assumes (i) isotropic UCN velocity distribution and (ii) gravity affects only the absolute value but not the angular distribution of UCN velocity

Geometry extrapolation

Neutron lifetime $$\tau_n^{-1} = \tau_1^{-1} - \left(\tau_2^{-1} - \tau_1^{-1}\right) / [\gamma_2(E)/\gamma_1(E) - 1]$$

is calculated using the measured lifetimes τ_1 and τ_2 for two UCN traps of different size and shape, provided the ratio of the UCN absorption rates γ_2 / γ_1 can be estimated.

1. Usual way:

$$\tau_{loss}^{-1}(E) = \frac{\int_0^{h_{\max}(E)} \bar{\mu}[E-h']\, v(E-h')\, \rho(E,h')\; dS(h)}{4\int_0^{h_{\max}(E)} \rho(E,h')\; dV(h)} \equiv \eta\gamma(E)$$

2. Oversimplified way:

$$\frac{\gamma_2(E)}{\gamma_1(E)} = \frac{S_2}{V_2} \Big/ \frac{S_1}{V_1}.$$

3. Exact calculation using Monte-Carlo or <u>another method</u> without any approximations. Usual Monte-Carlo calculations are still based on the assumption of isotropic velocity distribution at any height.

Rectangular UCN trap with mirror reflections from the walls allows analytical calculation of loss rate

The number of collisions with the walls during a long time $t \sim \tau_n \gg L_i/v_i$ can be easily estimated:

$$\mathcal{N}_x = tv_x/L_x,\ \mathcal{N}_y = tv_y/L_y,\ \mathcal{N}_z = tg/2v_z, \qquad (8)$$

The absorption probability during each collision is given by

$$\mu_i\left(v_i\right) = \frac{2\eta v_i/v_{\text{lim}}}{\sqrt{1 - v_i^2/v_{\text{lim}}^2}}.$$

The total absorption rate

$$\tau_a^{-1}\left(\mathbf{v}\right) = \sum_i \mu_i\left(v_i\right)\mathcal{N}_i/t.$$

Averaging over neutron direction gives UCN loss rate as a function of energy

$$\bar{\tau}_a^{-1}\left(v\right) = \int \tau_a^{-1}\left(\mathbf{v}\right)\, d\Omega/4\pi = \bar{\tau}_a^{-1}\left(E\right)$$

Rectangular UCN trap with mirror reflections from the walls allows analytical calculation of loss rate

1. Oversimplified method neglecting gravity effects

$$\tau_S^{-1}(E) = \frac{\eta g}{v_{\lim}} \frac{I_2(E_*)}{\sqrt{E_*}} (1 + 4h_* E_*)$$

2. Usual way

$$\bar{\tau}_a^{-1} = \frac{\eta g}{v_{\lim}} \frac{I_2(E_*)}{\sqrt{E_*}} \left\{ \frac{\arcsin\sqrt{E_*}}{I_2(E_*)} + 4h_* E_* \right\}$$

3. Exact calculation

$$\tau_g^{-1}(E) = \frac{3\eta g}{2v_{\lim}} \frac{I_2(E_*)}{\sqrt{E_*}} \left(1 + 4h_* \frac{I_1(E_*)}{I_2(E_*)} \right)$$

where

$$I_2(E_*) = \frac{1}{E_*}\left[\arcsin\sqrt{E_*} - \sqrt{E_*}\sqrt{1 - E_*}\right]$$

$$h_* = h_{\max}(L_x + L_y)/(2L_x L_y)$$

Energy dependence of UCN loss rate due to the absorption by trap bottom and side walls

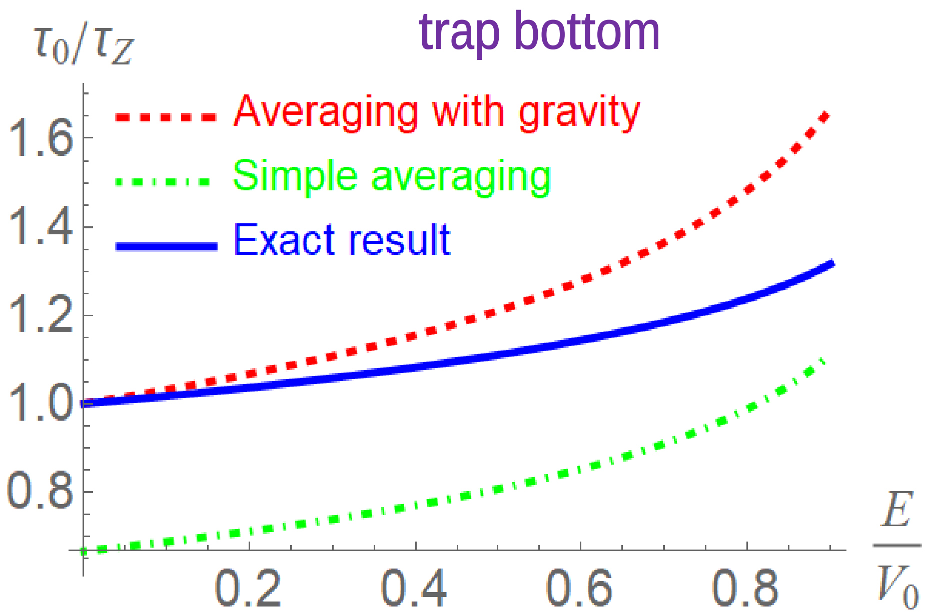

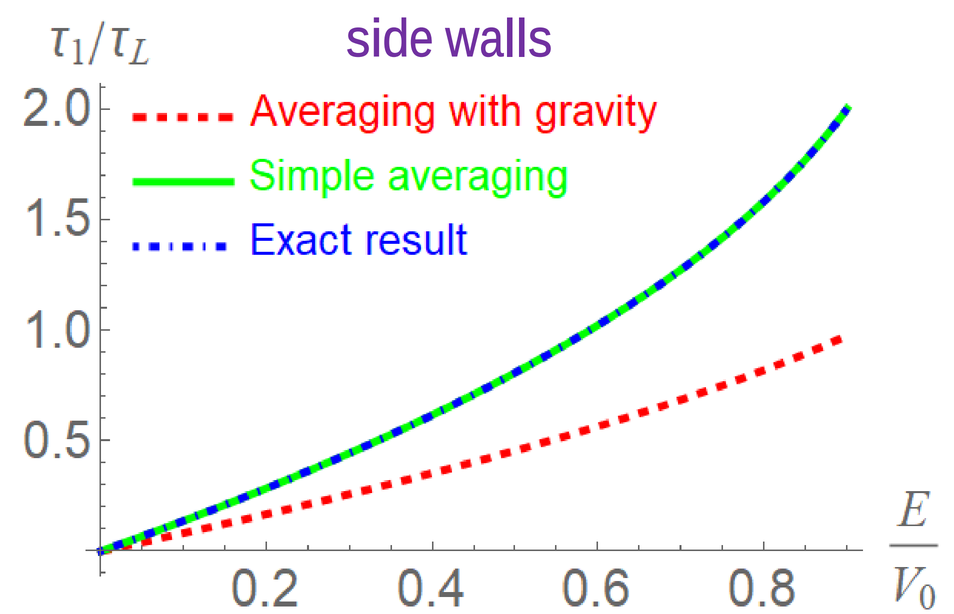

The absorption rate in a standard method is larger than in the exact calculation because the collision rate with trap bottom

$$\mathcal{N}_x = t v_x / L_x, \; \mathcal{N}_y = t v_y / L_y, \; \mathcal{N}_z = t g / 2 v_z$$

is smaller for faster neutrons, contrary to the standard formulas where the collision rate is always proportional to UCN velocity

The absorption rate in a standard method

$$\tau_{loss}^{-1}(E) = \frac{\int_0^{h_{\max}(E)} \bar{\mu}\left[E - h'\right] v\left(E - h'\right) \rho\left(E, h'\right) \, dS(h)}{4 \int_0^{h_{\max}(E)} \rho\left(E, h'\right) \, dV(h)}$$

is smaller than in the exact calculation because the collision rate with side walls is proportional to the horizontal UCN velocity, which does not decrease with height for a free neutron motion.

Energy dependence of UCN loss rate due to the absorption by trap bottom and side walls

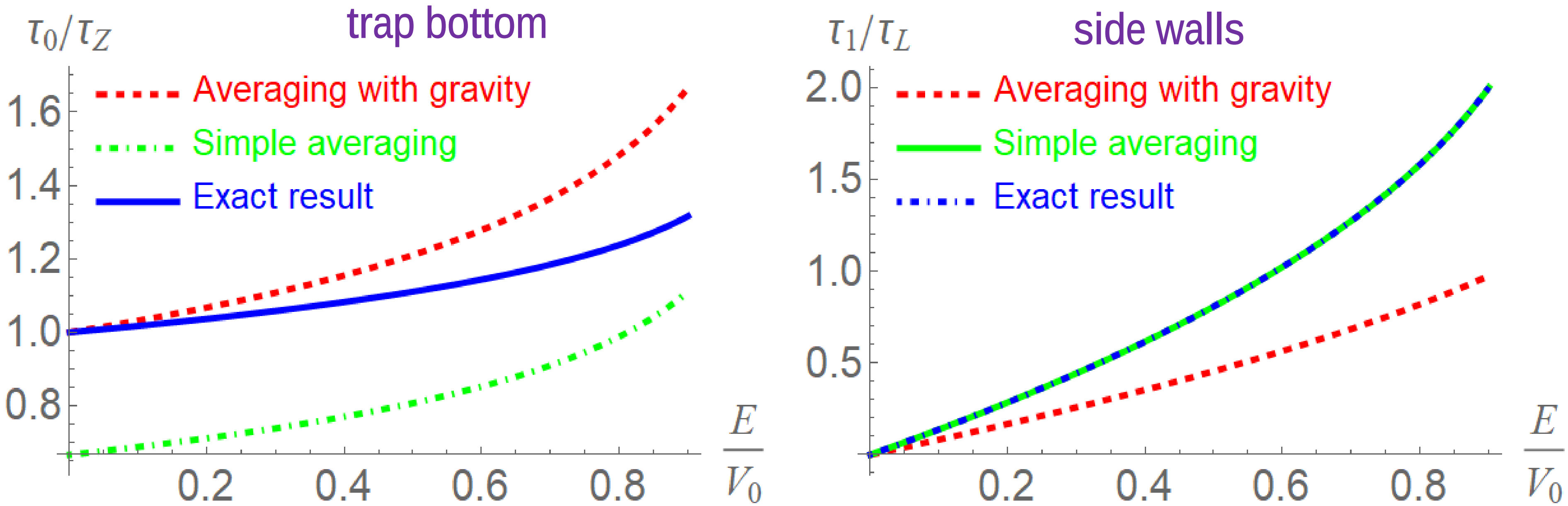

The UCN absorption rate and its dependence on UCN energy differ strongly for trap bottom and side walls. This means that the UCN absorption rate changes differently if the trap dimensions are reduced along the vertical z or horizontal x, y axes. This is very important because it affects the procedure of geometry extrapolation, on which all current precise τ_n measurements are based to account for the difference $\sim$ 2% between the measured and extracted neutron lifetime. Our calculations show that the result of this procedure depends strongly on the shapes of large and reduced UCN traps.

Results for geometrical scaling

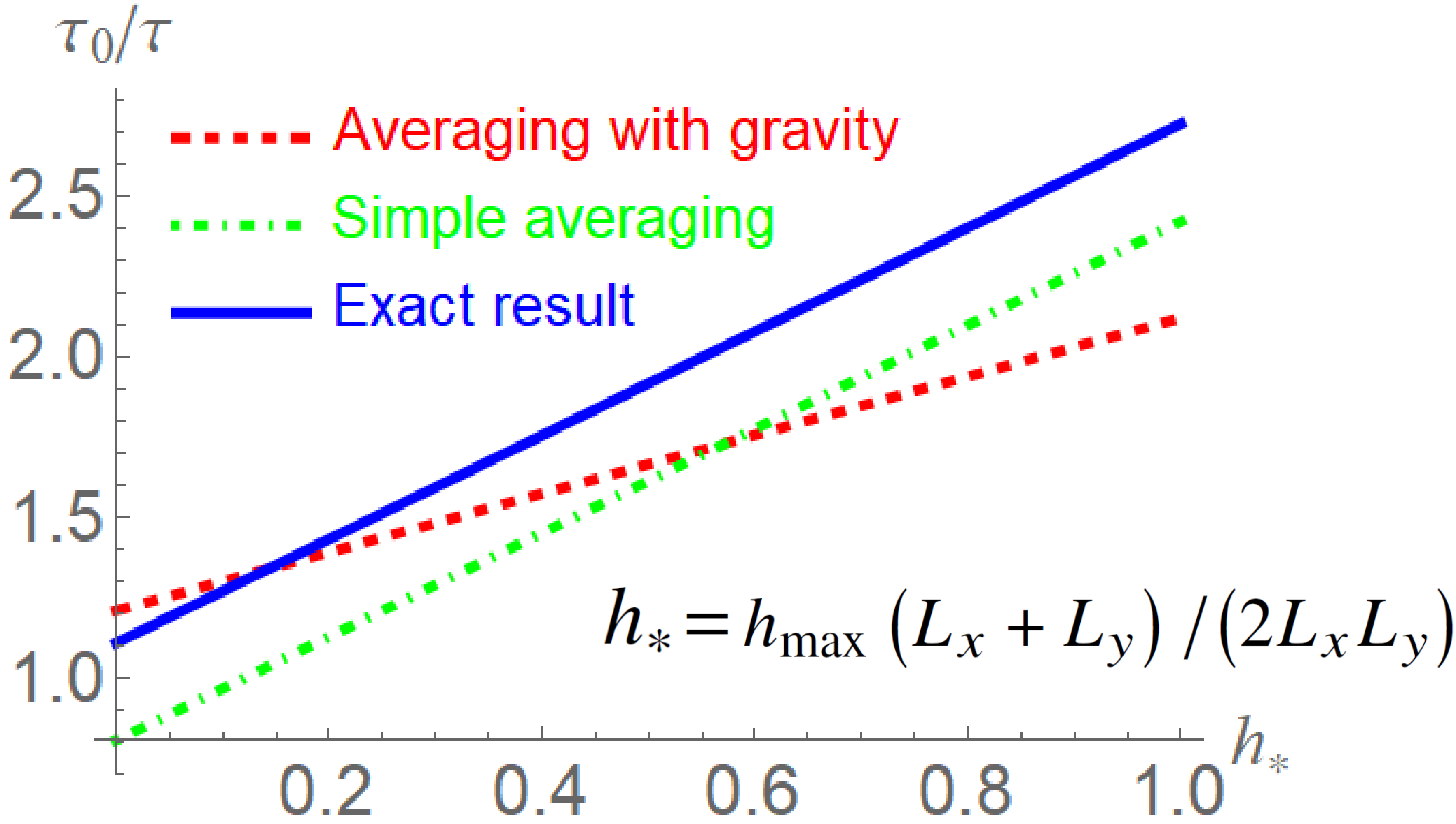

Our results can be easily generalized to UCN traps of the shape of straight cylinder with arbitrary base

Conclusions

1. Rectangular UCN trap with mirror reflections from the walls allows analytical calculation of UCN loss rate

2. We calculated the UCN absorption rate by trap walls using the standard (assuming an isotropic UCN velocity distribution at any height) and the exact methods.

3. Our results show that the geometry scaling and extrapolation to an infinite trap for extracting τ_n^{-1} must be done with a great care because the change of trap dimensions along the vertical and horizontal directions affects $\bar{\tau}_a^{-1}$ differently. Hence, the result of geometry extrapolation depends on the trap shape.

The work is supported by Russian Science Foundation grant #23-22-00312.

Thank you for attention!